SolarPACES 2023, 29th International Conference on Concentrating Solar Power, Thermal, and Chemical Energy Systems

Advanced Materials, Manufacturing, and Components

https://doi.org/10.52825/solarpaces.v2i.901

Published: 28 Aug. 2024

Effect of Load Cycling on High Temperature Creep of 316L Stainless Steel

Stuart Bell [1], Richard Clegg[1,2], Michael Cholette[1], Huy Truong-Ba[1], Geoffrey Will[3], and Ted Steinberg[1]

[1] Queensland University of Technology, Australia

[2] Explicom Engineering Investigators, Brisbane, QLD, Australia

[3] University of Sunshine Coast, QLD, Australia

*Correspondence: Stuart Bell, s2.bell@qut.edu.au

Abstract. For components in concentrating solar thermal plants, the creep mechanism will cause a significant portion of material damage to receivers, storage tanks, turbines and pipework. These components will undergo conditions where loads, temperature, or both load and temperature are not constatnly applied. This creep damage process will not resemble the constant load creep tests used to characterise creep of materials. Therefore, creep tests incorporating a load cycle were undertaken to obtain a better understanding of how high temperature materials respond to these cyclic conditions. These tests showed that when time under load was considered, creep undertaken under load cycling conditions were accelerated relative to constant load conditions. A modified Larson-Miller approach was used to assess this effect and determine an equivalent stress where constant load test data agrees with the cycled test data. This found that cycling the load was equivalent to if the system were under 3 and 7 MPa higher stress, for tests which were loaded for 12 hrs and 6 hrs per 24 hrs respectively. This could be a potential approach to simply and easily consider these load cycling effects for design and life analysis.

Keywords: Creep, Creep Damage, Load Cycling, Creep-Fatigue

1. Introduction

Concentrating solar thermal power plants will often produce creep damage to components such as receivers, storage tanks, turbines and even pipework. However, due to the daily cycle experienced by many of these components, this creep damage will not resemble the constant load creep testing which is used for design and life determination calculations. Many of these components will undergo conditions where loads, high temperature, or both load and temperature together are only experienced for a certain fraction of the total life in the component. As creep strain rates are a function of both load and temperature (i.e. $\dot{\gamma}=f(\sigma,T)$) [1], a better understanding of how high temperature materials respond to these cyclic conditions is required.

In order to explore how a commonly studied austenitic stainless steel responds to cycled load creep conditions, a set of tests were conducted where the load was applied and removed once per 24 hours, and held for varied time. The results of these tests were compared to the same material tested in a classic constant load creep test. The results were also analysed to determine effective creep curves whilst loaded, creep rates and projected creep life. Metallurgical analysis is also conducted to determine effects on the structure of the alloy.

2. Method

Creep tests were undertaken on a 100 kN Zwick Roell Kappa DS, fitted with a 3 zone high temperature furnace with thermocouples tied onto the sample and a temperature accuracy of ±1 °C. Temperature was measured and controlled using calibrated N type thermocouples in contact with the top and bottom of the test sample. Strain measurements were taken using a video extensometer with pattern tracking on the sample produced using alumina oxide powder, with an accuracy of 0.25 µm and a gauge length of 10 mm. Load was applied through pull rods and M12 threaded adapters to attach to the sample. The accuracy of this testing setup was validated by conducting testing using BCR-425 certified reference material and confirming that the creep rates and strains produced matched the certified values within the uncertainties allowed [2]. Samples were produced from 12.7 mm 316L bar acquired from Midway Metals, and machined to comply with ASTM E8 and ASTM E139, with a diameter of 6 ± 0.1 mm and a gauge length of 30 ± 0.1 mm.

Two sets of tests were undertaken at 750 °C. A first set or four tests using varying magnitudes of load but under constant load (i.e. no load cycle) was undertaken to characterize the creep behaviour of the material and determine an appropriate stress to conduct the cycled testing. Load cycled tests were undertaken at stresses between 95 MPa and 9.5 MPa for the loaded and unloaded case (i.e. a load ratio of 0.1). Minimum loads above zero were chosen to prevent shocking the sample with each load cycle and to maintain a consistent load when in the unloaded state. Three tests were undertaken, a constant load test, a test where the load was applied every 12 hours then unloaded for 12 hours, and a test where the load was applied for 6 hours and unloaded for 18 hours.

3. Results

3.1 Constant Load Creep Tests

The constant load creep curves presented in Figure 1 a) show very short primary and secondary creep stages and are dominated by the tertiary creep stage, which is common for stainless steels at these temperatures [2]. Minimum creep rate data is obtained by plotting the creep rates on a log-log plot as shown in Figure 1 b).

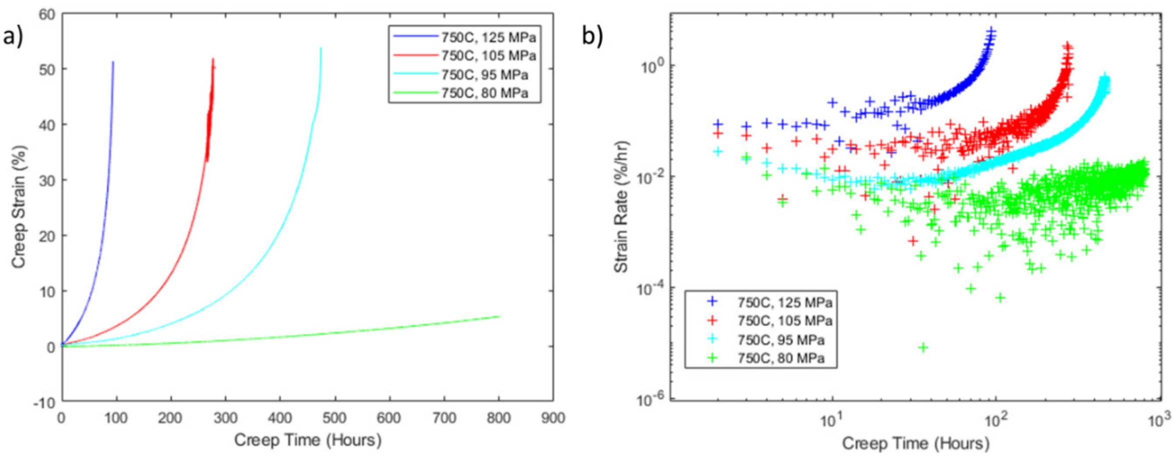

Figure 1. *a) Creep Curves and, b) Creep Rate log-log plot, for loads between 80 and 125 MPa at 750 °C*

From this data the minimum creep rates have been compared to those of other austenitic stainless steels obtained at 700 °C in Figure 2 (collated from a plot from [3]), particularly that obtained for 316L by Monteiro [4], Filacchioni [5] and Kloc [6], highlighted in orange, green and red respectively. A Norton stress exponent was also obtained from this data of

7.92 with an R2 fit of 99.85. This favourably compares to the other studies which have Norton Stress exponents around 7.5 to 8. This indicates that the creep mechanism investigated here is comparable to these previous studies at the lower temperature.

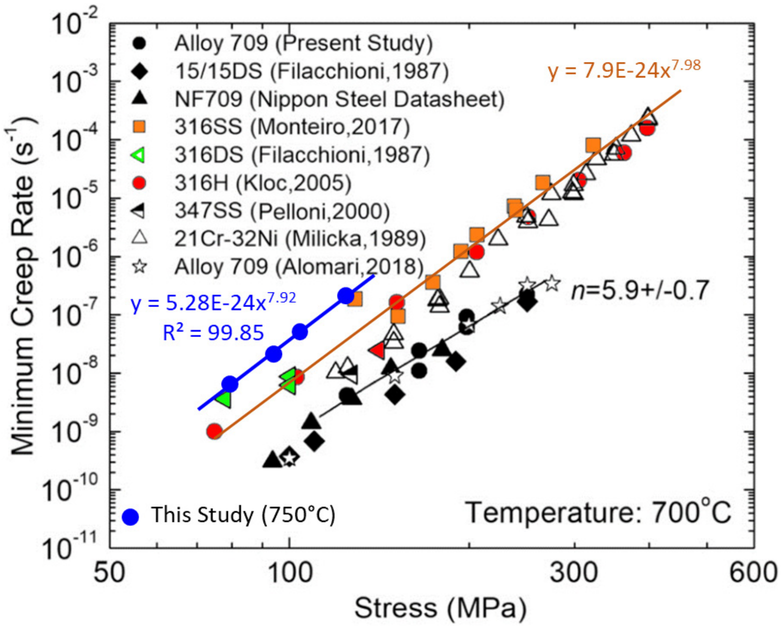

Figure 2. *Minimum Creep rate and Norton Stress Exponent compared to other studies. Plot modified from [3]*

3.2 Cycled Load Creep Tests

The creep curves from cycled load tests show that creep only occurs during the loaded portion of the curve. This is as would be expected. Therefore, the creep curves when plotted against total test time show significantly slower creep strain accumulation than the constant load test. However, closer inspection of these curves shows that the slope of the creep curve is greater than that of the constant load test at an equivalent time under load. When the unloaded time is removed from the plot, and the cycled tests are compared using time under load, this affect is obvious. The creep rates when loaded are significantly increased compared to a traditional, constant load creep test, as is shown in Figure 4.

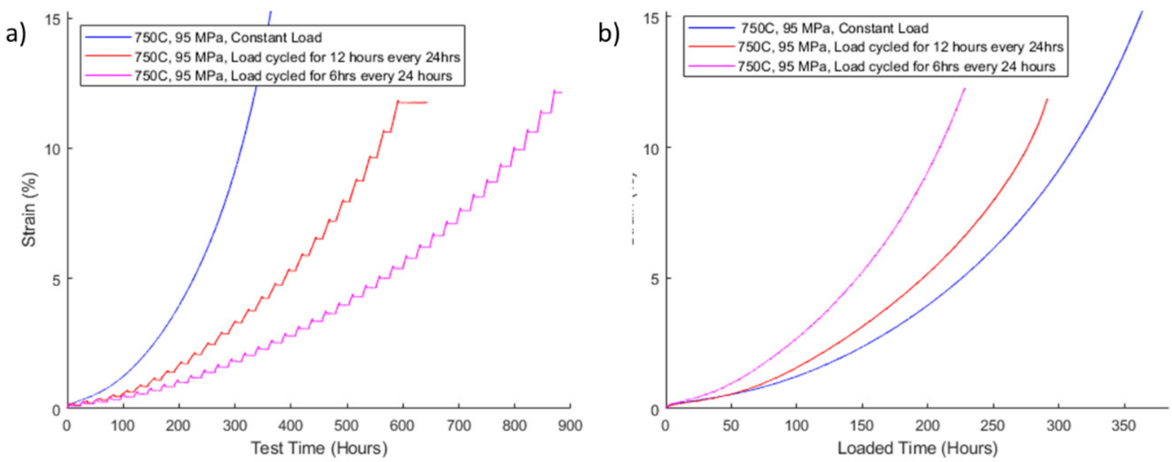

Figure 3. *Cycled load and constant load curves, a) compared total test time, b) compared to time loaded*

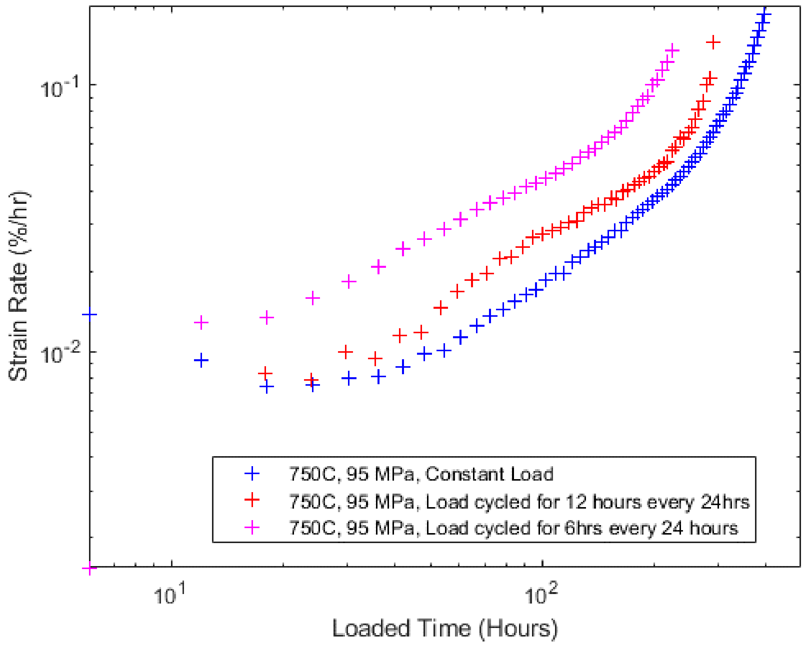

Figure 4. *Cycled load and constant load Creep Rate log-log plot*

3.3 Metallurgical analysis

In order to examine the microstructure of the samples, and particularly the presence of precipitates, samples were removed and sectioned before mounting in electroconductive resin (Struers Polyfast). The mounted samples were then polished with increasingly fine polishing compound up to ¼ um diamond paste to obtain a metallurgical finish. Samples were then imaged in Backscattered Electron mode using a TESCAN TIMA Field Emission Scanning Electron Microscope. Precipitate particles, which are likely embrittling sigma, chi and/or carbide phases [7], are easily distinguisable in backscattered SEM images as they are brighter due to their elevated molybdenum content. Images were analysed using ImageJ software to determine the area of the particles relative to the total area of the image. These measurements are summarised in Table 1, offering valuable insights.

Higher amounts of precipitate particles are present in the cyclic loaded samples. This is probably due to these samples experiencing longer test times and therefore time exposed to high temperatures. However, the nucleation and growth of precipites may be affected by the load history of the material. It is established that the cold work present in stainless steels will affect the nucleation and growth rate and type of precipitates produced [7]. However, the relationship between these factors is not well understood.

Low load areas (grip sections) see significant presence of precipitate particles along dislocation planes inside of grains. However, in high load areas the presence of precipitate particles inside of grains is reduced. This is likely due to the initial primary creep stage removing the dislocations from inside the grain and therefore reducing the number of nucleation sites for precipitation to initiate.

Table 1. *Precipitate area fraction determined by area analysis of bright particles in images.*

Test	**Section**	**Precipitate Area Fraction %**
Constant Load	Grip Section	1.59
	Gauge Section	1.93
12 hrs loaded/12 hrs unloaded	Grip Section	3.47

	Gauge Section	1.88
6 hrs loaded/18 hrs unloaded	Grip Section	4.08
	Gauge Section	2.73

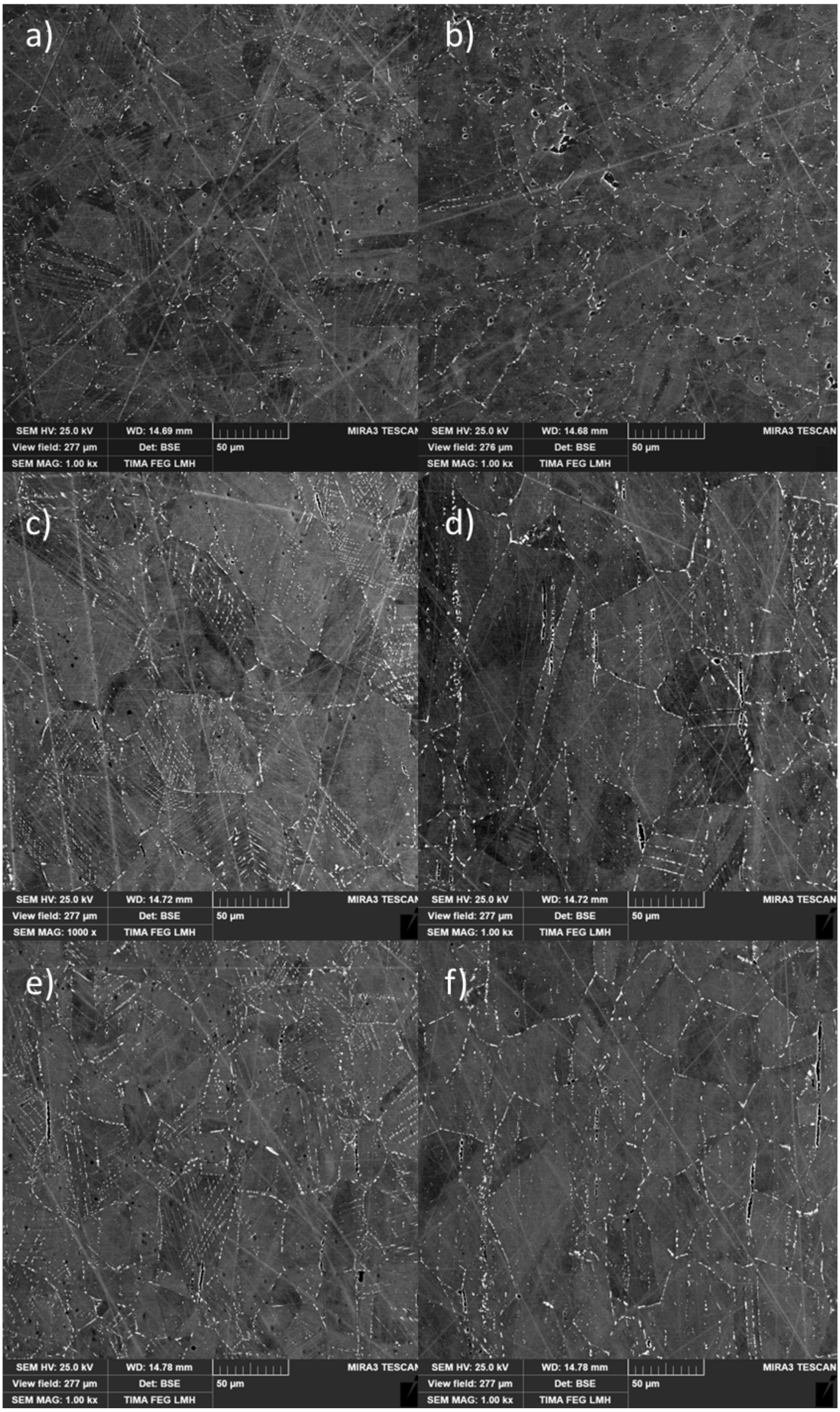

Figure 5. *Backscattered SEM images of a) constant load test, grip region (transverse section), b) constant load, gauge region (transverse section), c) 12 hrs loaded/12 hrs unloaded, grip region (longitudinal section), d) 12 hrs loaded/12 hrs unloaded, gauge region (longitudinal section), e) 6 hrs loaded/18*

hrs unloaded, grip region (longitudinal section), f) 6 hrs loaded/18 hrs unloaded, gauge region (longitudinal section). Load direction is orthogonal to the image in a) and b), but vertical in images c) through f).

3.4 Modelling

The constant load test data was analysed to determine the times to reach 1, 2 and 5%. This data was converted to a Larson-Miller parameter using:

$$P_{LM} = T.(C_{LM} + \log t_{strain})$$

Where P_{LM} is the Larson-Miller Parameter, T is the temperature in Kelvin, C_{LM} is the Larson-Miller Constant which was 20 in this case, and t_{strain} is the time to the strain being considered – i.e. 1, 2 and 5%.

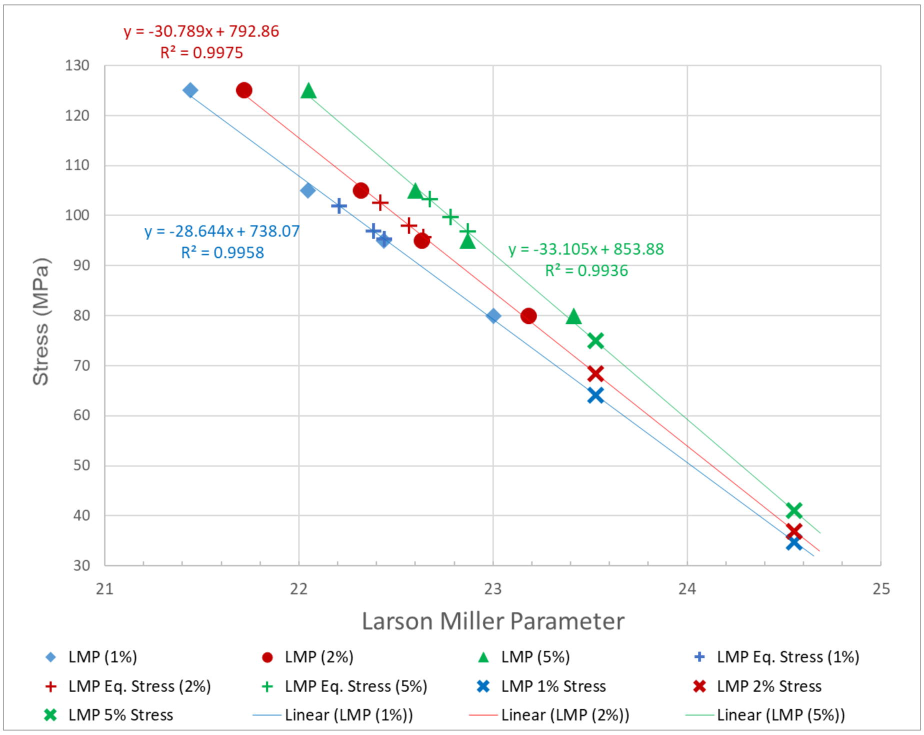

Figure 6. *Plot of Stress and Larson-Miller Parameter with extrapolated 1000 and 10 000 hr stress points and interpolated cycled load equivalent stress points.*

The Larson-Miller Parameter data is plotted on Figure 6, and linear lines of best fit for each strain are presented. These fitted functions are used to extrapolate the data to determine a 1000 hr and 10 000 hr stress for each strain line, represented by the × symbol in Figure 6. The stress values for these are tabulated in Table 2.

Table 2. *1000 and 10 000 hr stress values for 1%, 2% and 5% strain extrapolated using Larson-Miller Parameter.*

	1000 Hours	**10 000 Hours**
Stress for 1% Strain (MPa)	64.1	34.8
Stress for 2% Strain (MPa)	68.4	36.4
Stress for 5% Strain (MPa)	75.0	41.1

The next step was to use the Larson-Miller Parameter fit to provide a method to interpret with the increased strain curves found when the cycled tests are compared to loaded time. The time to reach the strains of interest for these cycled vs loaded time curves were used to find an equivalent stress which would produce those strains if it was under constant load conditions.

This interpolation is visually represented in Figure 6 using + symbols, while the corresponding data is tabulated in Table 3.

Table 3. *Equivalent stresses for cycled creep interpolated using Larson-Miller Parameter fitted data from the 1, 2 and 5% strains.*

Cycle Time (load/un-load)	LMP Eq. Stress (1%)	LMP Eq. Stress (2%)	LMP Eq. Stress (5%)
Constant	95.3	95.8	96.8
12/12 hrs	96.9	98.0	99.7
6/18 hrs	101.9	102.6	103.3

These results imply that, when considering time at load, load cycling increases the strain rate equivalent to a 3 and 7 MPa increase in constant load, for the 12/24 and 6/24 hours loaded respectively. This approach gives a potential method to simply and easily consider these effects for design and life analysis.

4. Summary

The testing conducted in this study indicates that there is a significant effect of the time in which this steel experiences elevated temperature without load on its creep behaviour. This produces elevated strain rates when loaded, compared to a more traditional constant load creep test. Therefore, the prediction of creep damage based off the most readily available creep data, from constant load testing, must be carefully applied or material life will be significantly overestimated. This may lead to early failure in materials which undergo cyclic conditions, a common situation in concentrating solar thermal power plant components.

However, if these elevated creep strains can be determined, some modifications to simple engineering tools already used for creep can be used in design calculations to more accurately determine creep life. This involves characterising the behaviour of the system using constant load tests to determine Larson-Miller Parameter information. Cycled load tests can then be undertaken to determine these strain rates. This information can be mapped against the Larson-Miller Parameter characteristics to determine an equivalent stress for a constant load system, which can be used for design purposes.

Future tests plan to explore other variables which will be experienced in various components in a CSP plant, and expand the tests to other high temperature materials such as 253MA stainless steel and 625 nickel alloy. Also, determining if these effects still occur at lower temperatures, which may be more relevant to components such as hot salt tanks is another goal. Another condition of interest would be to apply a consistent load but vary temperature. Not only would this condition allow the separation of load and temperature effects, it would be relevant to components under constant load but which experience temperature cycles, such as connectors and headers carrying the weight of a receiver. Additionally, cycling temperature and load together would enable the detection of combined effects, particularly relevant to components such as receiver tubes and dissimilar metal welds, which will have internal stresses produced from thermal gradients and temperature cycling.

Data availability statement

Data utilised to acquire the results in this study will be made available upon reasonable request.

Author contributions

Stuart Bell: Conceptualisation, Methodology, Investigation, Resources, Formal analysis, Data Curation, Writing - Original Draft, Writing - Review & Editing. **Richard Clegg**: Conceptualization, Methodology, Formal analysis. **Michael Cholette:** Conceptualization, Analysis, Resources. **Huy Truong-Ba:** Analysis. **Geoffrey Will**: Conceptualisation, Resources, Supervision, Funding acquisition, Writing - Review & Editing. **Theodore Steinberg**: Supervision, Funding acquisition.

Competing interests

The authors declare that they have no competing interests.

Funding

This research was performed as part of the Australian Solar Thermal Research Initiative (ASTRI), a project supported by the Australian Government, through the Australian Renewable Energy Agency (ARENA).

Acknowledgement

The data reported in the paper were obtained at the Central Analytical Research Facility (CARF) operated by the Institute for Future Environments at Queensland University of Technology (QUT). Access to CARF was supported by generous funding from the Faculty of Engineering.

References

1. M. Reith, et al, “Creep of Austenitic Steel AISI 316L(N),” Forschungzentrum Karlsruhe GmbH, Karlsruhe, Germany, 2004.
2. D. Gould, M. Loveday, “The certification of nimonic 75 alloy as a creep reference material,” Luxembourg, Commission of the European Communities, Directorate-General Science, 1990.
3. M. Taylor, et al., “Creep behavior of Alloy 709 at 700 °C” Mater. Sci. Eng. A, vol. 762, pp. 138083, Feb, 2019
4. S. N. Monteiro, et al., “Creep Parameters and Dislocation Substructure in AISI 316 Austenitic Stainless Steel From 600ºC to 800ºC,” Mater. Res., vol 20(Supp. 2), pp. 231-235, 2017
5. G. Filacchioni, “Tensile and creep behavior of a new family of austenitic alloys: the double stabilized stainless steels,” Mater. Nucl. React. Core Appl., vol 1, 191-198, 1987.
6. L. Kloc and J. Fiala, “Viscous creep in metals at intermediate temperatures,” Kov. Mater, vol. 43, no. 2, pp. 105-112, 2005.
7. B. Weiss and R. Stickler, “Phase Instabilities During High Temperature Exposure of 316 Austenitic Stainless Steel”, Metall. Trans., vol. 3, pp. 851-866, 1972.